

Theory of noise suppression in Λ -type quantum memories by means of a cavityJ. Nunn,^{1,*} J. H. D. Munns,^{1,2} S. Thomas,^{1,2} K. T. Kaczmarek,¹ C. Qiu,^{1,3} A. Feizpour,¹ E. Poem,^{1,4} B. Brecht,¹ D. J. Saunders,¹ P. M. Ledingham,¹ Dileep V. Reddy,⁵ M. G. Raymer,⁵ and I. A. Walmsley¹¹Clarendon Laboratory, University of Oxford, Parks Road, Oxford OX1 3PU, United Kingdom²QOLS, Blackett Laboratory, Imperial College London, London SW7 2BW, United Kingdom³Department of Physics, Quantum Institute for Light and Atoms, State Key Laboratory of Precision Spectroscopy, East China Normal University, Shanghai 200062, People's Republic of China⁴Department of Physics of Complex Systems, Weizmann Institute of Science, Rehovot 7610001, Israel⁵Oregon Center for Optical, Molecular and Quantum Science and Department of Physics, University of Oregon, Eugene, Oregon 97403, USA
(Received 1 January 2016; revised manuscript received 6 June 2017; published 31 July 2017)

Quantum memories, capable of storing single photons or other quantum states of light, to be retrieved on demand, offer a route to large-scale quantum information processing with light. A promising class of memories is based on far-off-resonant Raman absorption in ensembles of Λ -type atoms. However, at room temperature these systems exhibit unwanted four-wave mixing, which is prohibitive for applications at the single-photon level. Here, we show how this noise can be suppressed by placing the storage medium inside a moderate-finesse optical cavity, thereby removing the main roadblock hindering this approach to quantum memory.

DOI: [10.1103/PhysRevA.96.012338](https://doi.org/10.1103/PhysRevA.96.012338)**I. INTRODUCTION**

The need for low-loss active switching or synchronization of nondeterministic operations in a linear-optical quantum information processor has emerged over the past few years as a *sine qua non* for the development of large-scale photonics-based quantum technologies [1–5]. Experiments with optical switches are making rapid progress [6–9]. Quantum memories based on the coherent and reversible absorption of photons in an atomic ensemble are being developed by many groups as an alternative to optical switching [10–14], with impressive demonstrations of the preservation of quantum correlations and of temporal synchronization of photons, using cold atoms [15] and cold-doped crystals [16]. An important class of memory protocol is based on stimulated two-photon transitions in a Λ -type atomic ensemble, where a bright control laser field couples the incident signal photons to a ground-state coherence in the atoms [17]. Memories based on electromagnetically induced transparency (EIT) [18–20] and on far-off-resonant Raman absorption [21–23] both fall into this category, and in the following we will refer to all such memories as Λ memories. Λ memories in cold atoms have successfully stored single photons, but at room temperature it was found that fluorescence noise [24] and four-wave mixing [25] became problematic. Our group recently interfaced a single-photon source with a Raman memory and measured the photon number statistics of the retrieved fields [26]. There it was found that while fluorescence noise was negligible for off-resonant storage of short pulses, the thermal noise contributed by four-wave mixing destroyed the antibunching characteristic of single photons. Four-wave mixing noise is therefore the key roadblock preventing the implementation of Λ memories at room temperature [27,28]. Suggested solutions to this problem include partial suppression via polarization selection

rules [29], and engineering a Raman absorption feature in an isotopically mixed vapor [30]. In this paper, we consider the use of an optical cavity, enclosing the atoms, to suppress four-wave mixing noise.

It has been appreciated for some time that optical cavities provide a means to boost the interaction strength between light and atoms. Very high-finesse cavities enable near-deterministic storage with single atoms [31], but this is technically demanding and the cavity acceptance bandwidth is very narrow in this regime, which limits the suitability of such a memory for synchronizing photons generated by parametric scattering [3]. Working with atomic ensembles provides a collective enhancement of the atom-light coupling strength, such that the strong coupling regime of cavity QED is not required. The efficiency of cavity-enhanced light storage has been studied theoretically [32–34], though without considering four-wave mixing noise. Experimental achievements include a cavity-enhanced Duan-Lukin-Cirac-Zoller (DLCZ) type “emissive” quantum memory in cold atoms [35], and a demonstration of motional narrowing in a cavity-enhanced DLCZ setting using warm atoms [36], along with our own recent implementation of cavity-enhanced Raman storage in warm Cs vapor [37]. In this work, we present a theoretical analysis of this method of noise suppression, which is based on an alternative approach to deriving the response functions describing spontaneous scattering processes in a cavity. Our analysis is based on the method introduced in [38], which allows to drop the usual assumptions of low losses and high cavity finesse that underpin standard cavity input-output theory [39]. This allows us to directly predict the noise level (the average number of spontaneously scattered photons) and statistics (via the second-order autocorrelation) of the fields retrieved from the memory. We show that a moderate-finesse cavity, compatible with broadband operation, can suppress four-wave mixing noise to a low level. We also point out that the cavity-enhanced memory is nearly perfectly temporal-mode selective [40], making it an appealing system for chronocyclic encodings of quantum information [41].

*Present address: Centre for Photonics and Photonic Materials, Department of Physics, University of Bath, Bath BA2 7AY, United Kingdom.

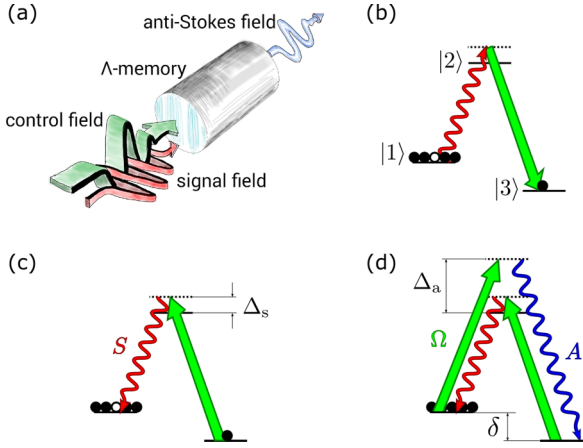


FIG. 1. (a) A control field (green) mediates the storage of a signal field (red) in a free-space Λ memory. The control field can drive the spontaneous Raman emission of an anti-Stokes field (blue) that generates a spurious excitation in the memory. (b) Atomic transitions driven in the storage interaction, (c) the retrieval interaction. (d) Four-wave mixing noise refers to the retrieval of the spurious excitation generated by the anti-Stokes scattering.

II. FOUR-WAVE MIXING IN Λ MEMORIES

Although the detailed dynamics in Λ memories differs depending on the protocol employed (EIT, Raman, Λ -GEM), all such memories share the same kinematical description, shown in Fig. 1. That is, an ensemble of Λ -type atoms are prepared in one of their two ground states, and then an incident signal field is coupled to the empty storage state by a strong control field tuned into two-photon resonance with the signal. Four-wave mixing arises in this system when the strong control field couples to the ground state and drives off-resonant spontaneous Raman scattering (in the diagram this is anti-Stokes scattering because we have chosen to pump the atoms into the higher of the two ground-state levels). The scattered anti-Stokes field is at a different frequency from the signal field and does not directly contribute any noise. But, each scattering event is accompanied by one of the atoms switching state from $|1\rangle$ to $|3\rangle$. That is, the scattering spontaneously generates excitations of the ground-state coherence that are indistinguishable from the excitations produced by successful storage of the signal field. When the memory is read-out, these excitations are retrieved as noise. The nomenclature “four-wave mixing” applies because there are four optical fields that coherently interact, even though they may not overlap in time. These are as follows: the control; the anti-Stokes; the control again; and finally the retrieved (noisy) signal.

III. SIMPLIFIED MODEL

Before running through the analysis in detail, we anticipate our main results by applying well-known results from the theory of cavities and etalons [42] to our cavity memory system. As shown in Fig. 2, we consider an atomic ensemble enclosed by a ring cavity with control and Stokes fields tuned into resonance with the cavity, and the anti-Stokes field tuned to

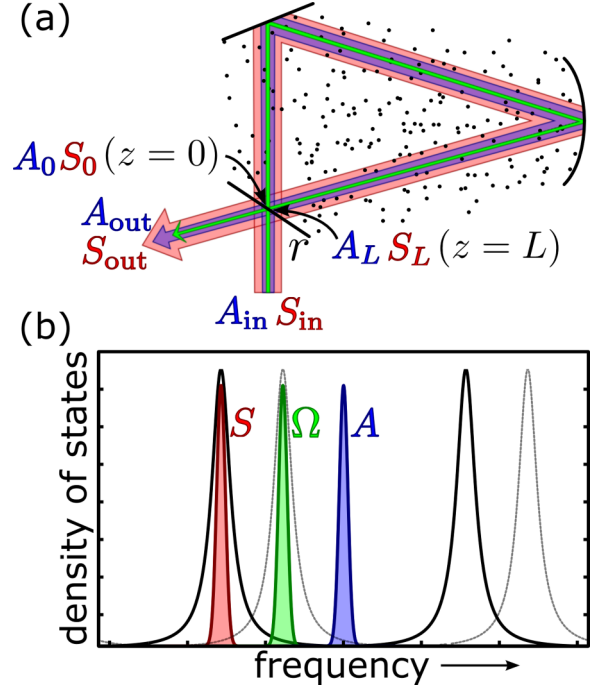


FIG. 2. (a) We model the dynamics of the cavity-enhanced Λ memory by considering the propagation of Stokes and anti-Stokes fields around a ring cavity through a storage medium comprising an ensemble of Λ -type atoms. The boundary conditions imposed by the input-output coupler with amplitude reflectivity r connects the intracavity fields to the incident and emitted fields. (b) The cavity resonances are tuned to suppress the density of scattering states (black peaks) at the anti-Stokes frequency with respect to the Stokes frequency. In our theoretical treatment, we allow arbitrary tuning of the Stokes and anti-Stokes fields with respect to the cavity resonances. By choosing the round-trip phases $\phi_s = 0$ (Stokes on resonance) and $\phi_a = \pi$ (antiresonant anti-Stokes), we achieve the optimal suppression depicted in the plot. Tuned midway between the Stokes and anti-Stokes frequencies, the control field can be resonantly coupled into the cavity in an orthogonal polarization mode (gray peaks) [37].

precise antiresonance (this could be achieved in a birefringent cavity with an orthogonally polarized control field [37]).

As described in the previous section, to successfully store and then retrieve an incident photon, we require Stokes absorption followed by Stokes emission [Figs. 1(b) and 1(c)], whereas the generation of a noise photon requires anti-Stokes emission followed by Stokes emission [Fig. 1(d)]. To obtain a conservative estimate for the noise level introduced by four-wave mixing, we consider the far-detuned limit, in which the cross sections for both Stokes and anti-Stokes scattering are equal. In that case, the only difference in strength between the desired and undesired interactions is provided by the cavity, which we arrange to preferentially select Stokes scattering over anti-Stokes scattering.

The density of optical states inside the ring cavity is determined by multiple interference and has the characteristic Airy-function shape, as depicted in Fig. 2(b). The signal-to-noise ratio (SNR) will be determined by the ratio of the peak ρ_{\max} to the minimum ρ_{\min} of the density of states. Operationally, this ratio $\rho_{\max}/\rho_{\min} = I_{\max}/I_{\min}$ can be measured directly by

probing the cavity with a tunable laser and detecting the leakage of light through one of the cavity mirrors, with the laser tuned first into resonance with the cavity to record I_{\max} , and then tuned to antiresonance to record I_{\min} . For a low-loss cavity, the ratio is given by [42]

$$\text{SNR} = \frac{I_{\max}}{I_{\min}} \approx \left(\frac{2\mathcal{F}_s}{\pi} \right)^2, \quad (1)$$

where \mathcal{F}_s is the cavity finesse for the signal field, which can also be measured directly via the cavity leakage spectrum, providing a consistency check.

For single-photon storage applications in optical quantum information processing, a key figure of merit is the $g^{(2)}$ autocorrelation function of the fields retrieved from the memory: noiseless single-photon Fock states exhibit perfect antibunching with $g^{(2)} = 0$, and the addition of noise is expected to pollute the photostatistics so that the two-photon probability is $p_2 \approx 1/\text{SNR}$, and the autocorrelation is then

$$g^{(2)} \approx \frac{2p_2}{p_1^2} \approx \frac{2}{\text{SNR}}. \quad (2)$$

Aside from suppressing noise, the cavity also enhances, but limits, the efficiency of the memory. As the optical fields make multiple passes through the atoms, the effective optical depth of the atomic vapor is increased. However, every round trip will inevitably incur some finite scattering loss, and these losses are also compounded over multiple round trips. First consider a ‘‘bulk memory’’, with no cavity.

In previous work [21] we showed that the single-pass far-detuned Λ -memory efficiency is parametrized by a coupling constant $C = \sqrt{Td\gamma}\Omega/\Delta$, where the control field has peak Rabi frequency Ω and duration T , the atomic vapor has optical depth d and homogenous resonance linewidth 2γ , and the signal field detuning from resonance is Δ . The overall memory efficiency scales with C^4 and unit efficiency can be achieved for $C^4 \gg 1$, which condition determines the control pulse energy $\mathcal{E} \propto \Omega^2 T$ required for efficient operation.

Now, for a cavity-enhanced Λ memory, we replace the single-pass optical depth d with the *cooperativity* $\mathcal{C} = d\mathcal{F}/\pi$, which is the optical depth achieved with an effective number of cavity round trips \mathcal{F}/π . Also, with a resonantly in-coupled control field as shown in Fig. 2(b), the intracavity field amplitude of the control is enhanced according to the Airy-distributed density of states, so that the control pulse energy is given by $\mathcal{E} \propto \Omega^2 T/\mathcal{F}_\Omega$, where \mathcal{F}_Ω is the cavity finesse for the control field. With these modifications, the control pulse energy required for optimal memory operation is reduced by $\mathcal{F}_s^2 \mathcal{F}_\Omega^2$, compared with a bulk, single-pass implementation without any resonant enhancement of the control.

On the other hand, losses in the cavity reduce the fraction of stored energy that can be retrieved. Just as losses limit the peak transmission of an etalon, so the maximum memory efficiency is limited by

$$\eta_{\text{tot}} \leq \left(\frac{\mathcal{F}}{\mathcal{F}_0} \right)^2, \quad (3)$$

where $\mathcal{F}_0 = \pi r/(1-r)$ is the ideal finesse of a lossless cavity, with r the amplitude reflectivity of the input-output coupler.

In the remainder of the paper, we present a more detailed analysis of the cavity-enhanced Λ memory, the results of which bear out these conclusions, although the resulting formulas are less transparent. We conclude with a discussion, where we connect the rigorous results to the expectations from the above simplified model.

IV. DETAILED MODEL

We now propose and analyze a scheme to inhibit four-wave mixing by using an optical cavity to modify the density of scattering states so that Stokes scattering is enhanced and anti-Stokes scattering is suppressed. That is, we tune the cavity into resonance with the Stokes frequency (this is also the frequency of the signal to be stored), whereas we ensure that the anti-Stokes frequency is antiresonant [Fig. 2(b)]. Below, we introduce a model that shows how four-wave mixing noise is suppressed by this arrangement.

We consider a Λ -memory storage medium with ground-state splitting δ placed inside a ring cavity¹ as shown in Fig. 2(a). Such a cavity can be successfully described with cavity input-output theory [39] and the operation of Λ memories in a cavity has been analyzed in this way [32]. However, cavity input-output theory is not suited to the description of fields tuned out of resonance with a cavity. To proceed, we instead follow the generalized input-output theory of Raymer and McKinstrie [38] and consider the traveling-wave propagation of the signal (Stokes) field S and the anti-Stokes field A around the ring cavity. The fields interact with the atomic ensemble in the presence of the control pulse, with Rabi frequency Ω , according to the linearized Maxwell-Bloch equations, which in the limit of a sufficiently smooth control, such that the excited state $|2\rangle$ can be adiabatically eliminated, take the form [43–45]

$$\begin{aligned} (c\partial_z + \partial_t)S &= ic\sqrt{\frac{d\gamma}{L}} \frac{\Omega}{\Gamma_s} B - \kappa_s S, \\ (c\partial_z + \partial_t)A &= ic\sqrt{\frac{d\gamma}{L}} \frac{\Omega}{\Gamma_a} B^\dagger - \kappa_a A, \\ \partial_t B &= -i\sqrt{\frac{d\gamma}{L}} \frac{\Omega^*}{\Gamma_s} S + i\sqrt{\frac{d\gamma}{L}} \frac{\Omega}{\Gamma_a} A^\dagger \\ &\quad - \left[\frac{1}{\Gamma_s} + \frac{1}{\Gamma_a} \right] |\Omega|^2 B, \end{aligned} \quad (4)$$

where the z -coordinate parametrizes the position along the folded optical path inside the cavity. The system (4) is to be interpreted as describing the evolution of the slowly varying annihilation operators S , A in the Heisenberg picture, with the bosonic spin-wave annihilation operator given by $B = \sum_{j \in [z, z+\delta z]} |1\rangle_j \langle 3|/\delta z \sqrt{N/L}$ describing the amplitude of the Raman coherence excited in the Λ memory.

¹The ring geometry simplifies the analysis to follow, but it also has the practical advantage that the intracavity fields are running waves without nodes at zero intensity. This ensures that atoms interacting with the fields during read-in do not escape interaction at retrieval by diffusing into the ‘‘dark’’ field nodes during the storage time.

The optical and spin-wave fields satisfy canonical commutation relations $[S(t, z), S^\dagger(t', z)] = [A(t, z), A^\dagger(t', z)] = \delta(t - t')$, $[B(t, z), B^\dagger(t, z')] = \delta(z - z')$. The operator nature of (4) is key to the analysis of spontaneous four-wave mixing noise. The meanings of the other symbols are as follows. $\Gamma_{s,a} = \gamma - i\Delta_{s,a}$ denotes the complex detuning of the signal and anti-Stokes fields from the atomic resonance with homogeneous linewidth 2γ . The complex decay rates $\kappa_{s,a}$ account for dispersion, absorption, and other scattering losses as the fields propagate. Strictly the losses in (4) should be accompanied by Langevin noise operators which maintain the bosonic commutation relations of the field operators [46]. But, vacuum noise entering due to losses experienced by the signal field does not contribute to the signal intensities or autocorrelations that we will compute, and anti-Stokes absorption and atomic decoherence are negligible in the Λ -memory configuration considered, thus we neglect Langevin forces [32]. The signal coupling strength is parametrized by the single-pass resonant optical depth d of the atomic ensemble, with N atoms in the signal beam path of length L [47]. Neglecting inhomogeneous broadening (generally valid far from resonance) the absorption and dispersion are given by

$$\kappa_s = \frac{d\gamma}{\tau\Gamma_s}; \quad \kappa_a = \frac{d\gamma}{\tau\Gamma_a^+}, \quad (5)$$

where $\Gamma_a^+ = \gamma - i(\Delta_a + \delta)$ is the complex detuning of the anti-Stokes field from the populated transition and $\tau = L/c$ is the cavity round-trip time. However, in an experiment the round-trip absorption and loss can be inferred from the cavity transmission spectrum [48]. Note that we have neglected decoherence of the spin wave since this is by assumption slow on the time scale of the memory interactions. The system (4) can be solved analytically [44], but in the limit that the interaction with the atoms is weak over the course of a single pass through the cavity, the fields A_L, S_L emerging from the interaction at $z = L$ can be related to the amplitudes S_0, A_0, B_0 at $z = 0$ by a Taylor expansion. To capture the round-trip dispersion and absorption precisely, we define $\tilde{S} = e^{\kappa_s z/c} S$, and similarly for the anti-Stokes, and obtain

$$\begin{aligned} S_L &\approx e^{-\kappa_s \tau} [\tilde{S}_0 + L \partial_z \tilde{S}|_{z=0}] \\ &= e^{-\kappa_s \tau} \left[S_0 + ic\tau \sqrt{\frac{d\gamma}{L}} \frac{\Omega}{\Gamma_s} B_0 - \tau \partial_t S_0 \right]; \\ A_L &\approx e^{-\kappa_a \tau} [\tilde{A}_0 + L \partial_z \tilde{A}|_{z=0}] \\ &= e^{-\kappa_a \tau} \left[A_0 + ic\tau \sqrt{\frac{d\gamma}{L}} \frac{\Omega}{\Gamma_a} B_0^\dagger - \tau \partial_t A_0 \right]. \end{aligned} \quad (6)$$

To capture the intracavity dynamics, we now ‘‘close the loop’’ by imposing as a boundary condition the beam-splitter relation at the input-output coupler, with amplitude reflectivity r (assumed real for simplicity):

$$\begin{aligned} S_0 &= r e^{ik_s L} S_L + t_r S_{\text{in}}, \\ A_0 &= r e^{ik_a L} A_L + t_r A_{\text{in}}, \end{aligned} \quad (7)$$

where $t_r = \sqrt{1 - r^2}$ is the input-output coupler amplitude transmission, k_s (k_a) denotes the signal (anti-Stokes) carrier wave vector, and we have introduced the input

field amplitudes $A_{\text{in}}, S_{\text{in}}$ impinging on the cavity from the outside. Substituting the solutions (6) into (7) we obtain

$$\begin{aligned} \partial_t s &= -\gamma_s s + i \sqrt{\frac{d\gamma}{\tau}} \frac{\Omega}{\Gamma_s} b + e^{-i\phi_s} \frac{t_r}{\mu_s \sqrt{\tau}} S_{\text{in}}, \\ \partial_t a &= -\gamma_a a + i \sqrt{\frac{d\gamma}{\tau}} \frac{\Omega}{\Gamma_a} b^\dagger + e^{-i\phi_a} \frac{t_r}{\mu_a \sqrt{\tau}} A_{\text{in}}, \\ \partial_t b &= i \sqrt{\frac{d\gamma}{\tau}} \left[-\frac{\Omega^*}{\Gamma_s} s + \frac{\Omega}{\Gamma_a} a^\dagger \right] - \left[\frac{1}{\Gamma_s} + \frac{1}{\Gamma_a^*} \right] |\Omega|^2 b, \end{aligned} \quad (8)$$

where we have defined the intracavity field amplitudes $a = \sqrt{\tau} A_0, s = \sqrt{\tau} S_0$, as in [38], and similarly $b = \sqrt{L} B_0$, and the resonant and antiresonant decay rates

$$\frac{1}{\gamma_{s,a}} = \tau \frac{\mu_{s,a} e^{i\phi_{s,a}}}{1 - \mu_{s,a} e^{i\phi_{s,a}}}, \quad (9)$$

where $\phi_{s,a} = k_{s,a} L - \text{Im}\{\kappa_{s,a}\}\tau$ is the cavity round-trip phase accumulated by the fields, including any dispersion induced by the atomic ensemble, and where the cavity round-trip amplitude transmission, including any atomic absorption, is given by $\mu_{s,a} = r e^{-\text{Re}\{\kappa_{s,a}\}\tau}$. If there are additional losses due to scattering from surfaces inside the cavity, or partial transmission through cavity mirrors, these can be incorporated into $\mu_{s,a}$. The system of coupled equations (8) takes a form that might be written using cavity input-output theory, except that we are able to treat the dynamics of both the Stokes and anti-Stokes fields, with one being resonant and the other off resonant with the cavity, as determined by the phases $\phi_{s,a}$.

V. BAD CAVITY LIMIT

To proceed to a solution, we once more invoke the bad cavity approximation, in which the fields impinging on the cavity are much more narrow band than the cavity linewidth [32]. Specifically, then, we require that $|\partial_t s| \ll |\gamma_s s|$, with commensurate bandwidths for the anti-Stokes and control fields. In this limit, we solve for s and a in terms of b by setting $\partial_t s = \partial_t a \approx 0$, to obtain

$$\begin{aligned} s &= i \sqrt{\frac{d\gamma}{\tau}} \frac{\Omega}{\Gamma_s \gamma_s} b + e^{-i\phi_s} \frac{t_r}{\gamma_s \mu_s \sqrt{\tau}} S_{\text{in}}, \\ a &= i \sqrt{\frac{d\gamma}{\tau}} \frac{\Omega}{\Gamma_a \gamma_a} b^\dagger + e^{-i\phi_a} \frac{t_r}{\gamma_a \mu_a \sqrt{\tau}} A_{\text{in}}, \\ \partial_t b &= \left\{ \frac{d\gamma}{\tau} \left[\frac{1}{\Gamma_s^2 \gamma_s} + \frac{1}{|\Gamma_a|^2 \gamma_a^*} \right] - \frac{1}{\Gamma_s} - \frac{1}{\Gamma_a^*} \right\} |\Omega|^2 b \\ &\quad + i \frac{t_r \sqrt{d\gamma}}{\tau} \left[\frac{\Omega^*}{\mu_s \Gamma_s \gamma_s} e^{-i\phi_s} S_{\text{in}} + \frac{\Omega}{\mu_a \Gamma_a \gamma_a^*} e^{i\phi_a} A_{\text{in}}^\dagger \right]. \end{aligned} \quad (10)$$

At this point, it is convenient to remove the dependence on the temporal shape of the control field by making a coordinate transformation $t \rightarrow \epsilon(t) = \int_{-\infty}^t |\Omega(t')|^2 dt' / W$, with W chosen so that $\epsilon(\infty) = 1$. Then, we have $\partial_t = W^{-1} |\Omega(t)|^2 \partial_\epsilon$ [17,21]. Defining normalized signal and anti-Stokes field amplitudes $\sigma = s \sqrt{W} / \Omega$ and $\alpha = a \sqrt{W} / \Omega$, the system (10)

becomes

$$\begin{aligned}\sigma &= c_s b + p_s \sigma_{\text{in}}, \\ \alpha &= c_a b^\dagger + p_a \alpha_{\text{in}}, \\ \partial_\epsilon b &= f b + g_s \sigma_{\text{in}} + g_a \alpha_{\text{in}}^\dagger,\end{aligned}$$

where we pulled the various constants into the coefficients

$$\begin{aligned}c_{s,a} &= i \sqrt{\frac{d\gamma W}{\tau}} \frac{1}{\Gamma_{s,a} \gamma_{s,a}}, \\ p_{s,a} &= \frac{t_r e^{-i\phi_{s,a}}}{\mu_{s,a} \gamma_{s,a} \sqrt{\tau}}, \\ f &= W \left[\frac{d\gamma}{\tau} \left(\frac{1}{\Gamma_s^2 \gamma_s} + \frac{1}{|\Gamma_a|^2 \gamma_a^*} \right) - \frac{1}{\Gamma_s} - \frac{1}{\Gamma_a^*} \right], \\ g_s &= i \frac{t_r e^{-i\phi_s} \sqrt{d\gamma W}}{\mu_s \Gamma_s \gamma_s \tau}; \quad g_a = i \frac{t_r e^{i\phi_a} \sqrt{d\gamma W}}{\mu_a \Gamma_a \gamma_a^* \tau}.\end{aligned}\quad (11)$$

Note that the above transformations are unitary so the operators α , σ , b obey the canonical relations $[\alpha, \alpha^\dagger] = [\sigma, \sigma^\dagger] = [b, b^\dagger] = 1$. Solving for b gives

$$b(\epsilon) = b(0) e^{f\epsilon} + \int_0^1 d\epsilon' M_c(\epsilon, \epsilon') \{g_s \sigma_{\text{in}}(\epsilon') + g_a \alpha_{\text{in}}^\dagger(\epsilon')\}, \quad (12)$$

where we have defined $M_c(\epsilon, \epsilon') = \Theta(\epsilon - \epsilon') M(\epsilon, \epsilon')$ as the causal version of the cavity response function $M(\epsilon, \epsilon') = e^{f[\epsilon - \epsilon']}$, with Θ denoting the Heaviside step function.

Now, we are ready to solve for the outgoing fields emerging from the cavity, using again the beam-splitter boundary conditions at the input-output coupler:

$$\begin{aligned}S_{\text{out}} &= t_r e^{ik_s L} S_L - r S_{\text{in}}(t), \\ A_{\text{out}} &= t_r e^{ik_a L} A_L - r A_{\text{in}}(t).\end{aligned}\quad (13)$$

In the limit of weak single-pass coupling, we can approximate (6) by $e^{ik_s L} S_L \approx (\mu_s/r) e^{i\phi_s} S_0$, retaining only the phase evolution and losses of the Stokes field as it traverses the cavity.² Substituting this into (13) and using (10), the output field, switching back to the normalized variables $\sigma_{\text{in,out}} = S_{\text{in,out}} \sqrt{W}/\Omega$, is found to be

$$\sigma_{\text{out}} = \frac{it_r (\mu_s/r) e^{i\phi_s} \sqrt{d\gamma W}}{\Gamma_s \gamma_s \tau} b + [\chi - r] \sigma_{\text{in}}, \quad (14)$$

where we have defined the cavity transmission amplitude

$$\chi = \frac{t_r^2}{r} \frac{\mu_s e^{i\phi_s}}{1 - \mu_s e^{i\phi_s}}. \quad (15)$$

VI. STORAGE AND RETRIEVAL

We consider first the field emerging from the cavity when we attempt to store an incident signal. This field will contain both a contribution from the unstored signal due to the finite efficiency of the storage interaction, and also a contribution

from four-wave mixing noise. Assuming for simplicity that the memory is initially prepared with no spin-wave excitations,³ the output field is found from (14) and (12) to be

$$\sigma_{\text{out},1}(\epsilon) = \int_0^1 d\epsilon' \{M_1(\epsilon, \epsilon') \sigma_{\text{in},1}(\epsilon') + M_{\text{FWM}}^{[1]}(\epsilon, \epsilon') \alpha_{\text{in},1}^\dagger(\epsilon')\}, \quad (16)$$

where we have defined the integral kernels

$$\begin{aligned}M_1(\epsilon, \epsilon') &= -\chi C_s^2 M_c(\epsilon, \epsilon') + (\chi - r) \delta(\epsilon - \epsilon'); \\ M_{\text{FWM}}^{[1]}(\epsilon, \epsilon') &= -\chi C_s C_a x M_c(\epsilon, \epsilon'),\end{aligned}\quad (17)$$

where the subscript 1 indicates fields associated with the storage interaction. Here, we have introduced the signal and anti-Stokes memory coupling parameters

$$C_{s,a} = \frac{\sqrt{\mathcal{C}\gamma W}}{\Gamma_{s,a}}, \quad (18)$$

with $\mathcal{C} = d\mu_s e^{i\phi_s}/(1 - \mu_s e^{i\phi_s})$ the cooperativity of the cavity for the signal field. On resonance with the cavity ($\phi_s = 0$), this is equal to the optical depth of a medium with length $L \times \mathcal{F}_s/\pi$, where \mathcal{F}_s is the cavity finesse for the signal field (when the control field Ω is not present). Note that the coupling of the anti-Stokes field is multiplied by the *noise suppression factor*

$$x = \frac{\mu_s e^{i\phi_s} \gamma_s}{\mu_a e^{-i\phi_a} \gamma_a^*} = \frac{1 - \mu_s e^{i\phi_s}}{1 - \mu_a e^{-i\phi_a}}. \quad (19)$$

This is the factor that we will aim to minimize by appropriate tuning of the cavity resonances.

We next consider the retrieval interaction. In this case, there is no incident signal field, and the initial spin wave is (neglecting decoherence during storage) given by the excitation generated at read-in, so that the retrieved signal field can be written as

$$\begin{aligned}\sigma_{\text{out},2}(\epsilon) &= \int_0^1 d\epsilon' \{M_2(\epsilon, \epsilon') \sigma_{\text{in},1}(\epsilon') + M_{\text{FWM}}^{[2]}(\epsilon, \epsilon') \alpha_{\text{in},1}^\dagger(\epsilon') \\ &\quad + M_{\text{FWM}}^{[1]}(\epsilon, \epsilon') \alpha_{\text{in},2}^\dagger(\epsilon')\},\end{aligned}\quad (20)$$

where we have defined the integral kernels

$$\begin{aligned}M_2 &= -\chi C_s^2 e^f M; \\ M_{\text{FWM}}^{[2]} &= -\chi C_s C_a x e^f M \\ &= (\Gamma_s/\Gamma_a) x M_2.\end{aligned}\quad (21)$$

Here, we have assumed for convenience in simplifying the expressions that the control pulse used to drive the retrieval interaction is identical to the storage control pulse.

²Note that reusing the Taylor expansion in (6) actually exacerbates the truncation error of the weak-interaction approximation and gives an incorrect result for (14).

³For memories based on alkali-metal vapors, Rb or Cs, this requires efficient optical pumping of the atomic ensemble into one of the two hyperfine states within its ground-state manifold. In practice, this is hard to achieve, but fortunately experiments have shown that a small residual population of unpumped atoms does not significantly affect the operation of the memory [26].

VII. EFFICIENCY AND NOISE

The above expressions provide a means to predict the efficiency of the memory by comparing the expectation values $N_x = \langle \int_{-\infty}^{\infty} S_x^\dagger(t) S_x(t) dt \rangle = \langle \int_0^1 \sigma_x^\dagger(\epsilon) \sigma_x(\epsilon) d\epsilon \rangle$ of the input and output intensity operators ($x = \text{in, out, 1, 2}$). Four-wave mixing noise enters via the operators describing the incident anti-Stokes fields, which, although they are in the vacuum state (we do not send in any anti-Stokes light), nonetheless contribute to the intensity because the incident fields are described by creation operators, giving rise to anti-normally-ordered terms. In a noiseless memory one would define the total efficiency $\eta_{\text{tot, noiseless}} = N_{\text{out,2}}/N_{\text{in,1}}$, with commensurate definitions for the storage efficiency $\eta_{\text{store, noiseless}} = 1 - N_{\text{out,1}}/N_{\text{in,1}}$ and the retrieval efficiency $\eta_{\text{ret, noiseless}} = \eta_{\text{tot, noiseless}}/\eta_{\text{store, noiseless}}$. For a noisy memory we modify the definition of the total efficiency by subtracting the noise floor $N_{\text{out,2}}|_{\text{no input}}$ retrieved from the memory when $N_{\text{in,1}} = 0$ (no incident signal photons):

$$\eta_{\text{tot}} = \frac{\tilde{N}_{\text{out,2}}}{N_{\text{in,1}}}; \quad \tilde{N}_{\text{out,2}} = N_{\text{out,2}} - N_{\text{out,2}}|_{\text{no input}}. \quad (22)$$

In computing these expectation values, it is helpful to adopt matrix notation for the integral kernels, so that for a two-dimensional function $K = K(\epsilon, \epsilon')$, we can write $\int_0^1 K(\epsilon, \epsilon') K^*(\epsilon'', \epsilon') d\epsilon'$ simply as $KK^\dagger = KK^\dagger(\epsilon, \epsilon'')$, and $\int_0^1 K(\epsilon, \epsilon') \psi(\epsilon') d\epsilon'$ simply as $K|\psi\rangle$, where the ket notation is unrelated to the quantum mechanics of the problem, but is used to denote the vectorized version of the function $\psi(\epsilon)$. In this notation, the trace is given by $\text{tr}\{K\} = \int_0^1 K(\epsilon, \epsilon) d\epsilon$. With these preliminaries, we can write the transmitted and retrieved photon numbers, for the case of input coherent state or Fock state signal fields, as

$$N_{\text{out},j} = \text{tr}\{P_j\},$$

where we have defined the operators

$$P_j = N_{\text{in},1} |\varphi_j\rangle \langle \varphi_j| + \sum_{k=1}^j M_{\text{FWM}}^{[k]} M_{\text{FWM}}^{[k]\dagger}, \quad (23)$$

with $|\varphi_j\rangle = M_j |\psi_{\text{in}}\rangle$, and $\psi_{\text{in}}(\epsilon)$ the mode function describing the temporal amplitude of the input signal field, normalized so that $\langle \psi_{\text{in}} | \psi_{\text{in}} \rangle = 1$. To see how this works, consider the temporal amplitude of the signal field emerging from the storage interaction

$$\varphi_1(\epsilon) = -\chi C_s^2 e^{f\epsilon} \psi(\epsilon) + (\chi - r) \psi_{\text{in}}(\epsilon),$$

where $\psi(\epsilon) = \int_0^\epsilon e^{-f\epsilon'} \psi_{\text{in}}(\epsilon') d\epsilon'$. The number of photons, including noise due to four-wave mixing, is then found to be

$$N_{\text{out,1}} = N_{\text{in,1}} \langle \varphi_1 | \varphi_1 \rangle + |\chi C_s C_a x|^2 \frac{1-E}{\zeta},$$

where we have defined $E = \int_0^1 e^{-\zeta\epsilon} d\epsilon = (1 - e^{-\zeta})/\zeta$, with the dimensionless coupling parameter ζ given by

$$\begin{aligned} \zeta &= -(f + f^*) \\ &= -2 \text{Re}\{C_s^2 + C_a^2 x(\mu_a/\mu_s) e^{-i(\phi_s + \phi_a - 2 \arg \Gamma_a)}\} \\ &\quad + 2W \text{Re}\left\{\frac{1}{\Gamma_s} + \frac{1}{\Gamma_a^*}\right\}. \end{aligned} \quad (24)$$

Considering now the retrieval interaction, the temporal mode emerging from the memory is

$$\varphi_2(\epsilon) = -\chi C_s^2 e^{f\epsilon} (e^\zeta E)^{1/2} \kappa e^{f\epsilon},$$

where we have introduced the normalized overlap between the input field and the cavity response, $\kappa = (e^\zeta E)^{-1/2} \psi(1)$. With this definition, when $\psi_{\text{in}}(\epsilon) \propto e^{f^*\epsilon}$, we obtain $\kappa = 1$. Including the contributions from four-wave mixing, the number of photons retrieved from the memory is found to be

$$N_{\text{out,2}} = |\chi C_s|^2 [|C_s E \kappa|^2 N_{\text{in,1}} + |C_a x|^2 g(\zeta)], \quad (25)$$

where we defined $g(\zeta) = (1 - e^{-\zeta} E)/\zeta$. The first term describes the coherent operation of the memory; the second term describes the retrieval of noise photons that are present even when no signal photons are sent into the memory. The efficiency of the memory is seen to be

$$\eta_{\text{tot}} = |\chi C_s^2 E \kappa|^2. \quad (26)$$

Taking the ratio of the first and second terms in (25) provides the following formula for the signal-to-noise ratio (SNR) of the memory:

$$\text{SNR} = N_{\text{in,1}} |\kappa|^2 \times \left| \frac{\Gamma_a}{\Gamma_s} \right|^2 \times \frac{E^2}{g(\zeta)} \times \frac{1}{|x|^2}. \quad (27)$$

Parsing this result from left to right, the SNR increases with the number of incident signal photons, and with the degree to which they overlap with the cavity response, described by $|\kappa|^2$. The second factor is essentially the ratio of the anti-Stokes and Stokes detunings, which factor is also present in a cavityless Λ memory. This reflects the fact that low-noise operation can be achieved with detunings much smaller than the splitting between the ground states of the Λ system, as can be realized with EIT in cold atoms [49]. The third factor is purely dynamical, but the final factor, proportional to $|x|^{-2}$, represents the noise suppression afforded by the cavity. As should now be clear, minimizing $|x|$ by appropriate tuning of the cavity resonances provides a route to low-noise operation of a Λ memory, even at room temperature where large detunings from resonance are necessary. Note that for a single far-detuned ideally mode-matched incident photon, with the cavity tuned as in Fig. 2(b) with the anti-Stokes field on antiresonance $\phi_a = \pi$ and the Stokes field on resonance $\phi_s = 0$, and noting that $\mu_s \approx \mu_a \sim 1$, we find

$$x \approx \frac{\pi}{2\mathcal{F}_s} \quad (28)$$

recover the ‘‘intuitive’’ expression derived in Eq. (1), up to the numerical factors E^2/g , which emerge from the detailed dynamics.

VIII. MODE SELECTIVITY

The cavity memory interaction is a single-mode interaction. That is to say, the memory stores just a single temporal mode, and a single temporal mode is retrieved from the memory [50]. This is clear from the structure of the solution (20), where the coherent mapping between input and output is described by the Green’s function $M_2 \propto M = e^{f[\epsilon - \epsilon']}$, which is a *separable* function of ϵ and ϵ' . Accordingly, the efficiency of the memory is parametrized by the overlap

integral κ defined above; any input mode orthogonal to $e^{-f\epsilon}$ will not couple to the memory at all. Furthermore, converting back into the ordinary time coordinate $\psi_{\text{in}}(t) = W^{-1/2}\Omega(t)\psi_{\text{in}}[t(\epsilon)]$, we observe that the input mode that is stored can be arbitrarily chosen by appropriate shaping of the control field Ω . The single-mode nature of the cavity memory interaction has been derived previously, albeit without considering four-wave mixing [32,51], but here we point out that it is an advantageous feature. The combination of single-mode operation and arbitrary shaping has been dubbed *temporal mode selectivity*, and is a useful feature for quantum optical information processing, where large-alphabet signals can be demultiplexed by a mode-selective “drop filter” [40]. In fact, the conventional traveling-wave Raman protocol [21,47] is nearly single mode [52], but the mode selectivity degrades at high efficiency, a phenomenon encountered also in engineering mode-selective frequency conversion [53]. Recently, Reddy *et al.* showed how to achieve high-mode selectivity and high efficiency in frequency conversion by double passing or multipassing the active medium, so that each interaction was weak enough to remain effectively single mode [54,55]. The perfect mode selectivity of the cavity memory analyzed here can be understood as the multipass limit of this approach, where the interaction describing a single pass through the cavity is weak, and therefore separable, whereas the coherent combination of all cavity round trips provides for arbitrarily high efficiency while retaining temporal-mode selectivity.

IX. AUTOCORRELATION

A key figure of merit for the operation of a quantum memory is the ability to preserve the sub-Poissonian statistics of stored single-photon Fock states. In our recent experiments with a Raman Λ memory without any cavity, we found that although the average number of noise photons generated by four-wave mixing in the absence of an input signal field was low, the effect of four-wave mixing on the photon statistics of the fields retrieved from the memory was dramatic [26]. To see how the cavity influences the performance of the memory as a component for synchronizing photonic quantum information, we compute the $g^{(2)}$ autocorrelation function for the fields emerging from the memory, which can be written as

$$g_{\text{out},j}^{(2)} = \frac{\int_0^1 \int_0^1 d\epsilon d\epsilon' \langle \sigma_{\text{out},j}^\dagger(\epsilon) \sigma_{\text{out},j}^\dagger(\epsilon') \sigma_{\text{out},j}(\epsilon') \sigma_{\text{out},j}(\epsilon) \rangle}{\left[\int_0^1 d\epsilon'' \sigma_{\text{out},j}^\dagger(\epsilon'') \sigma_{\text{out},j}(\epsilon'') \right]^2} = 1 + \frac{\text{tr}\{P_j^2\} - (2 - g_{\text{in},1}^{(2)})N_{\text{in},1}^2 \langle \varphi_j | \varphi_j \rangle^2}{N_{\text{out},j}^2}. \quad (29)$$

For the fields emerging from the storage interaction, we obtain the result

$$N_{\text{out},1}^2 [g_{\text{out},1}^{(2)} - 1] = [g_{\text{in},1}^{(2)} - 1] N_{\text{in},1}^2 \langle \varphi_1 | \varphi_1 \rangle^2 + \text{tr}\{M_{\text{FWM}}^{[1]} M_{\text{FWM}}^{[1]\dagger} M_{\text{FWM}}^{[1]} M_{\text{FWM}}^{[1]\dagger}\} + 2N_{\text{in},1} \langle \varphi_1 | M_{\text{FWM}}^{[1]} M_{\text{FWM}}^{[1]\dagger} | \varphi_1 \rangle, \quad (30)$$

where the second term evaluates to

$$\text{tr}\{M_{\text{FWM}}^{[1]} M_{\text{FWM}}^{[1]\dagger} M_{\text{FWM}}^{[1]} M_{\text{FWM}}^{[1]\dagger}\} = |\chi C_s C_a x|^4 \zeta^{-4} \{4\zeta(1-E) - 2\zeta^2 E - \Sigma\}, \quad (31)$$

with $\Sigma = 2e^{-\zeta}[\sinh(\zeta) - \zeta]$. Of particular interest is the corresponding expression for the $g^{(2)}$ autocorrelation of the fields retrieved from the memory by the readout control pulse, which, after some rather lengthy calculations, can be written as

$$N_{\text{out},2}^2 [g_{\text{out},2}^{(2)} - 1] = |\chi C_s|^4 \{ [g_{\text{in},1}^{(2)} - 1] N_{\text{in},1}^2 |C_s E \kappa|^4 + |C_a x|^4 h(\zeta) + 2N_{\text{in},1} |C_s C_a x \kappa|^2 h'(\zeta) \}, \quad (32)$$

where we defined the functions

$$h(\zeta) = 4 \frac{1-E}{\zeta^3} - 2 \frac{E}{\zeta^2} + E^4 + \frac{\Sigma}{\zeta^4} (2\zeta E - 1),$$

$$h'(\zeta) = E^4 + \frac{E\Sigma}{\zeta^3}. \quad (33)$$

For the case of storing single-photon Fock states, for which $g_{\text{in},1}^{(2)} = 0$, we obtain

$$g_{\text{out},2}^{(2)} = \{2N_{\text{in},1} |\kappa C_s C_a x|^2 [E^2 g(\zeta) + h'(\zeta)] + |C_a x|^4 [g(\zeta)^2 + h(\zeta)]\} \times [N_{\text{in},1} |\kappa C_s E|^2 + |C_a x|^2 g(\zeta)]^{-2}.$$

Note that for incident single photons, $N_{\text{in},1} \leq 1$ is to be interpreted as the average number of photons per pulse, including any losses prior to the memory. For a heralded photon source [56], $N_{\text{in},1}$ is therefore the *heralding efficiency* of the source.

If we achieve strong noise suppression, so that $|x|^2 \ll N_{\text{in},1}$, then the autocorrelation can be written as

$$g_{\text{out},2}^{(2)} = 2 \left[1 + \frac{h'(\zeta)}{E^2 g(\zeta)} \right] \frac{1}{\text{SNR}}. \quad (34)$$

We note that the first term in this expression is the same as predicted by our simple model in Eq. (2). However, the more complete analysis is required for a quantitative prediction, and to see how the autocorrelation changes with the coupling strength of the memory interaction.

X. WEAK COUPLING LIMIT

The expressions for the efficiency, signal-to-noise ratio, and autocorrelation simplify in the limit of weak coupling, when $|C_{s,a}| \ll 1$, so that $\zeta \ll 1$. In this limit we obtain, to first order in ζ (valid for $\zeta \lesssim 0.2$), $E \rightarrow 1 - \frac{1}{2}\zeta$, $\Sigma \rightarrow \frac{1}{3}\zeta^3 - \frac{1}{3}\zeta^4$, $g(\zeta) \rightarrow \frac{3}{2} - \frac{7}{6}\zeta$, $h(\zeta) \rightarrow \frac{11}{6} - \frac{13}{5}\zeta$, $h'(\zeta) \rightarrow \frac{4}{3} - \frac{5}{2}\zeta$. The number of retrieved photons is then given by

$$N_{\text{out},2} = |\chi C_s|^2 \left[N_{\text{in},1} (1 - \zeta) |C_s \kappa|^2 + \left(\frac{3}{2} - \frac{7}{6}\zeta \right) |C_a x|^2 \right],$$

with the efficiency given by

$$\eta_{\text{tot}} = (1 - \zeta) |\chi C_s^2 \kappa|^2,$$

and the signal-to-noise ratio

$$\text{SNR} = \left(\frac{2}{3} - \frac{4}{27}\zeta \right) N_{\text{in},1} |\kappa|^2 \left| \frac{\Gamma_a}{\Gamma_s} \right|^2 \frac{1}{|x|^2}.$$

The autocorrelation (again for incident single photons in the high noise-suppression regime) is found to be

$$g_{\text{out},2}^{(2)} = \left(\frac{34}{9} - \frac{14}{81} \zeta \right) \frac{1}{\text{SNR}}. \quad (35)$$

In general, the control field $\Omega(t)$ can be shaped so as to achieve $|\kappa| = 1$ and maximize the SNR. In the weak coupling limit, the requirement to shape the signal and control pulses is relaxed because when $|f| \ll 1$, the optimal input mode $e^{f^* \epsilon}$ is approximately flat. If the signal and control pulse shapes derive from a common source, so that $\psi_{\text{in}}(t) \propto \Omega(t)$ and $\psi_{\text{in}}(\epsilon) = 1$, we then achieve $\kappa = 1 - \frac{3}{2}f - \frac{1}{4}f^* \approx 1$.

XI. STRONG COUPLING

On the other hand, it is also instructive to consider the case of very strong coupling, when $\zeta \gg 1$. Note that the size of ζ depends on the signal field frequency through the phase ϕ_s , so this limit depends on the control field energy, optical depth, and also on the signal field tuning. With $\zeta \gg 1$, we have $E \rightarrow 1/\zeta$, $g(\zeta) \rightarrow 1/\zeta$, $\Sigma \rightarrow 1$, $h(\zeta) \rightarrow 2(\zeta - 1)/\zeta^4$, $h'(\zeta) \rightarrow 2/\zeta^4$, and the memory efficiency tends to

$$\begin{aligned} \eta_{\text{tot}} &\rightarrow \left| \frac{\chi C_s^2 \kappa}{\zeta} \right|^2 \\ &= |\chi \kappa|^2 \frac{|C_s|^4}{\zeta^2}. \end{aligned} \quad (36)$$

For very strong coupling, we find $g_{\text{out},2}^{(2)} \rightarrow 1$, independent of the noise suppression factor x . In this case, the four-wave mixing gain dominates and the system has effectively become a Raman laser. To remain in the regime where the cavity suppresses the four-wave mixing, we should have $|x| \ll N_{\text{in},1}/\zeta$, in which case from (34) we obtain

$$g_{\text{out},2}^{(2)} = \left| \frac{\Gamma_s}{\Gamma_a} \right|^2 \frac{2|x|^2 \zeta}{N_{\text{in},1} |\kappa|^2}.$$

Here, the autocorrelation rises linearly with the coupling parameter ζ . To achieve low-noise operation of the memory, we therefore seek the smallest coupling strength ζ for which the efficiency saturates. Note that the above result, derived from a detailed analysis, is the same as we expect from our simple model, for the case of a single far-detuned ideally mode-matched incident photon, in Eq. (2), except it is larger by a factor of ζ , and of course $\zeta \gg 1$ by assumption, in the strong coupling regime.

XII. COMPARISON WITH PREVIOUS RESULTS

Cavity-enhanced Λ memories have been analyzed previously [32–34]. To compare with those works, we consider the case that there is no four-wave mixing (equivalent to the limit $\delta \rightarrow \infty$ so that $C_a = 0$), and we assume the signal field to be tuned to the empty-cavity resonance with $k_s L = 0 \pmod{2\pi}$. Finally, we assume that there are no interface or scattering losses inside the cavity, other than atomic absorption contained in κ_s , and we assume that the single-round-trip dispersion and absorption is small, $|\kappa_s| \tau \ll 1$. In this case, we can express the cooperativity \mathcal{C} for the signal field in terms

of the absorption-free cooperativity $\mathbb{C} = rd/(1-r)$,

$$\mathcal{C} \approx \mathbb{C} \frac{1}{r} \frac{\Gamma_s}{\Gamma_{\mathbb{C}}}, \quad (37)$$

where $\Gamma_{\mathbb{C}} = \Gamma_s + \mathbb{C}\gamma$. We also find $\zeta \approx 2W\gamma(\mathbb{C} + 1)/|\Gamma_{\mathbb{C}}|^2$, $\chi \approx (1+r)\Gamma_s/\Gamma_{\mathbb{C}}$, and $C_s^2 \approx W\gamma\mathbb{C}/\Gamma_s\Gamma_{\mathbb{C}}$, which upon substitution into (36) yields the rather elegant result, previously derived by Gorshkov [32], that the optimal storage efficiency in the limit of strong coupling is

$$\eta_{\text{tot}} = |\kappa|^2 \left(\frac{1+r}{2} \right)^2 \left[\frac{\mathbb{C}}{\mathbb{C}+1} \right]^2, \quad (38)$$

which is independent of the detuning Δ_s and also independent of the control field energy $\mathcal{E} \propto W$, provided the control field is strong enough to reach saturation, $\zeta \gg 1$. Unit efficiency is achieved with an optically thick ensemble in a high-quality cavity with a mode-matched storage interaction such that $|\kappa| = 1$.

In a real atomic system, four-wave mixing is present, and in that case the maximum noise suppression is achieved when the cavity resonance condition $\phi_s = 0 \pmod{2\pi}$ obtains, which is different to the empty-cavity resonance condition $k_s L = 0 \pmod{2\pi}$ assumed above, because of atomic dispersion. In fact, the resonance condition $\phi_s = 0$ is natural in a real experiment, where the atoms are introduced into the cavity before the signal field is tuned to resonance with the cavity. Any other scattering losses inside the cavity should also be included in the round-trip amplitude transmission μ_s . Four-wave mixing gain can boost the efficiency (while introducing noise), whereas intracavity losses will reduce the efficiency. In general, the expression (26) and its strong coupling limit (36) can be used to predict the memory performance.

XIII. BANDWIDTH

The analysis presented here assumes adiabatic following of the atoms driven by the intracavity fields, and also adiabatic evolution of the intracavity fields driven by the external fields impinging on the cavity. In fact, Eqs. (8) hold generally, for arbitrary pulse bandwidths (consistent with adiabatic following of the atomic dynamics), but the subsequent closed-form solutions require the *bad cavity* approximation, which holds when the spectral bandwidth of the external fields is much narrower than the decay rates $\gamma_{s,a}$ of the intracavity fields. Equivalently, the cavity resonance at the signal frequency, with linewidth γ_s , should be broad compared to the signal pulse bandwidth. In this limit, the acceptance bandwidth δ_s of the memory is constrained by the cavity finesse $\delta_s < a \Delta_{\text{FSR}}/\mathcal{F}_s$, where $a \sim 0.3$ is a “safety margin” and where Δ_{FSR} is the free spectral range of the cavity. Assuming low loss so that $\mu_a \approx \mu_s \approx 1$, and the resonance and antiresonance conditions $\phi_s = 0 \pmod{2\pi}$, $\phi_a = \pi \pmod{2\pi}$, we have $x \approx 2\pi/\mathcal{F}_s$, and so $\delta_s \propto x$, which expresses a tradeoff between noise suppression and speed of operation.

It is worth pointing out that the conventional relationship, used above, between the cavity finesse on the one hand, and its acceptance bandwidth on the other, is not fundamental, but arises from the linear relation between intracavity phase and optical carrier frequency in a nondispersive medium. White-light cavities use anomalous dispersion to remove the overall

frequency dependence of the intracavity phase over a broad bandwidth [57]. To design a cavity-enhanced Λ memory with simultaneously broad bandwidth and high-noise suppression, one could imagine a related but inverted design principle: a broadband cavity with a dispersive element that accelerates the accumulation of phase at frequencies close to the unwanted anti-Stokes, such that they are pushed out of resonance with the cavity. One could, for example, replace one of the internal cavity mirrors with a Gires-Tournois interferometer (GTI), which is simply another ring cavity that reflects all incident optical power, but with a phase shift that depends strongly on the detuning from its resonant frequencies. With this design, a very broadband memory cavity could be used, that would accept a broadband input pulse. Without the GTI, the anti-Stokes would not experience the greatest possible noise suppression as it would still be partially resonant with the cavity. But with the GTI, one can arrange that the anti-Stokes field picks up a significant phase shift on reflection, such that its cavity round-trip phase is $\phi_a = \pi$ and it is strongly suppressed. A full analysis of this design lies beyond the scope of this work, but here we simply note that this and other designs are possible, which circumvent the noise and speed tradeoff discussed above.

XIV. SPATIAL MODES

We have treated the evolution of the fields in the cavity by considering the one-dimensional propagation equations (4). Of course, spontaneously initiated four-wave mixing may populate any spatial mode; the important point as a source of noise for the Λ -memory interaction is whether a spontaneously scattered photon is associated with a spin-wave excitation that can be retrieved into the signal mode as noise. For emission events that scatter anti-Stokes photons out of the cavity, it is clear by momentum conservation that retrieval into the cavity from the resulting spin wave is not phase matched. For paraxial scattering events, one should consider the density of states at the anti-Stokes frequency for higher-order transverse cavity modes. Such events populate spin waves with transverse spatial structure, and these may couple in some degree to the signal in the fundamental cavity mode due to the transverse structure of the control field [58]. The main contribution will be from scattering into transverse modes that are resonant with the anti-Stokes frequency. Higher-order Hermite-Gaussian modes with mode index p are detuned from the fundamental cavity mode ($p = 0$) by $p\xi$, where ξ is a frequency offset determined by the Guoy phase [42]. In order to align the cavity, we assume that it has been designed such that the frequency offset is larger than the cavity linewidth, $\xi \gtrsim \text{FSR}/\mathcal{F}$, so that the spatial modes are spectrally distinct. The cavity-based noise suppression fails for the spatial mode for which the anti-Stokes frequency, by assumption tuned halfway between the fundamental cavity modes, is on resonance. This fixes the index of this failure mode as $p_{\text{fail}} \approx (\text{FSR}/2)/\xi \approx \mathcal{F}/2$. The probability P to retrieve this excitation into the fundamental cavity mode depends on the intermode coupling mediated by the control field, which we assume to be coupled into the fundamental cavity mode (possibly with an orthogonal

polarization to the signal field),

$$P \propto \left| \int U_0(x)^2 U_{p_{\text{fail}}}(x) dx \right|^2,$$

where the mode profile is given by $U_p(x) = N_p h_p(\sqrt{2}x)e^{-x^2}$, with h_p the Hermite polynomial of degree p and N_p a normalization. We find numerically that $P \lesssim 10^{-p_{\text{fail}}/2}$, and thus noise due to paraxial anti-Stokes scattering into higher-order cavity modes is suppressed by a factor exponential in the cavity finesse.

XV. CAVITY-ENHANCED RAMAN MEMORY

Here, we consider a specific implementation of a Λ memory in caesium vapor, in the far-off-resonant Raman limit. While our results are valid for adiabatic storage with arbitrary detunings, and also on resonance (which corresponds to EIT-type Λ memories), the Raman configuration has the advantage that broadband pulses can be stored at room temperature outside of the Doppler and collisional absorption profile, and the pulse durations \sim ns time scale are sufficiently short that the collisional fluorescence [24] and dephasing are negligible during the optical interactions [59]. Preliminary experiments have confirmed the operating principles of the cavity-enhanced memory proposed here [37], and this calculation indicates that a high-performance memory is within reach. We begin by noting the caesium hyperfine splitting of $\delta = 9.2$ GHz $= 57.8 \times 10^9$ s $^{-1}$. For simplicity, consider the proposal, mentioned above, to use a tunable birefringence to in-couple an orthogonally polarized control field. Neglecting for the moment atomic dispersion, this fixes the free-spectral range of the cavity to $\Delta_{\text{FSR}} = 4\delta/(2m + 1)$, where the integer $m = 0, 1, 2, \dots$ specifies the *order* of the cavity, that is, the number of cavity resonances that lie between the signal and anti-Stokes frequencies. The largest operating bandwidth is achieved for the largest free-spectral range, so we consider a zero-order cavity. The cavity round-trip length is then fixed to be $L = 2\pi c/\Delta_{\text{FSR}} = 8$ mm, which is much smaller than a comparable free-space memory and could be incorporated “on chip”. The natural linewidth of the Cs D_2 line at $\lambda = 852$ nm is $2\gamma = 5.2$ MHz, but with a buffer gas to extend the storage lifetime the pressure-broadened linewidth could be larger, so we will assume $2\gamma \approx 50$ MHz. We then choose a signal detuning of $\Delta_s = 5$ GHz, which puts us in the far-off-resonant limit, and which lies sufficiently outside the Doppler profile, ~ 500 MHz at room temperature, that inhomogeneous broadening of the vapor can be neglected. Assuming a temperature of $\sim 70^\circ\text{C}$, the optical depth, fixed by the cavity length L and the temperature dependence of the caesium vapor pressure, is found to be $d \approx 380$. For a collimated cavity mode, the Rayleigh range should be matched to the round-trip length, which fixes the transverse mode area to $\mathcal{A} = \lambda L$. Figure 3 shows the efficiency and $g^{(2)}$ autocorrelation function for the storage of single photons heralded with efficiency $N_{\text{in},1} = 0.5$ in such a cavity-enhanced Raman memory, as a function of the energy of the control pulses, for two different input-output coupler reflectivities, and assuming several different levels of intracavity loss. We consider ideal mode matching such that the mode overlap is $|\kappa| = 1$.

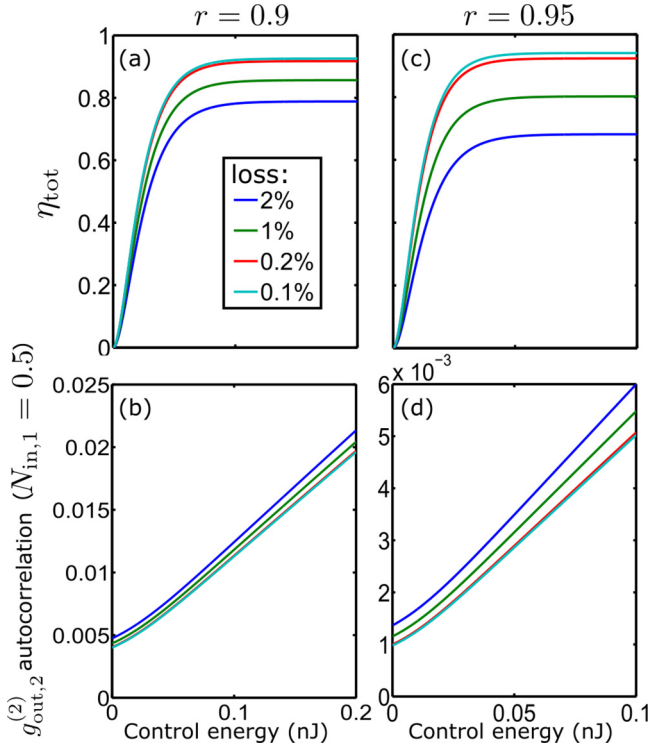


FIG. 3. The predicted efficiency η_{tot} and autocorrelation $g_{\text{out},2}^{(2)}$ for the storage of single photons, heralded with efficiency $N_{\text{in},1} = 0.5$, in a cavity-enhanced Raman memory, as described in the text, with input-output coupler reflectivities $r = 0.9$ [(a),(b)] and $r = 0.95$ [(c),(d)], and a range of intracavity round-trip intensity losses (see legend).

The cavity linewidth is 1.3 and 0.6 GHz for the two cases $r = 0.9$ and 0.95 , respectively. The memory acceptance bandwidths are then $\delta_s \sim 400$ and 200 MHz, respectively. These are compatible with cavity-enhanced down-conversion sources [60] and would enable the storage of few-ns-duration pulses, suitable for the fastest useful clock rates, $\sim 0.1 - 1$ GHz, for electronic synchronization applications. Finally, the control pulse energies required to saturate the efficiency, on the order of $\mathcal{E} = 10$ pJ, are sufficiently low that the memory could be driven by the modulated output of a semiconductor diode laser.

XVI. ASYMPTOTIC EFFICIENCY WITH FINITE LOSS

As can be seen in Fig. 3, in each case the efficiency saturates at an asymptotic value determined by the intracavity loss. This is predicted by the formula in Eq. (36), noting that in the far-detuned Raman case with strong noise suppression, we have $\zeta \approx 2|C_s|^2$, so that, setting $N_{\text{in}} = |\kappa| = 1$ for an ideally mode-matched single photon,

$$\eta_{\text{tot}} = \left| \frac{\chi}{2} \right|^2.$$

This reduces to the prediction in Eq. (3), equivalent to the maximum efficiency of a lossy Gires-Tournois interferometer, if we note that on resonance with $\phi_s = 0$, we have

$$\chi = (1-r)(1+r) \frac{\mu_s/r}{1-\mu_s}$$

$$\begin{aligned} &\approx 2 \times \left(\frac{\mu_s}{1-\mu_s} \right) / \left(\frac{r}{1-r} \right) \\ &= 2 \frac{\mathcal{F}_s}{\mathcal{F}_0}. \end{aligned} \quad (39)$$

Given some finite cavity losses $\alpha = \mu_s/r$, the efficiency is maximized by setting the input-output coupler reflectivity to be

$$r_{\text{opt}} = \frac{1 - \sqrt{1 - \alpha^2}}{\alpha}.$$

For the case of a Raman-type memory considered here, even with lossless optical components, off-resonant absorption contributes a loss $\alpha \approx e^{-d(\gamma/\Delta_s)^2}$, which, using the above optimal reflectivity, imposes the efficiency limit

$$\eta_{\text{tot}} \leq 1 - 2\sqrt{2} \frac{\gamma\sqrt{d}}{\Delta_s}.$$

XVII. CONCLUSION

We have described a method to suppress four-wave mixing noise in a Λ memory by means of a cavity tuned simultaneously into resonance with the signal field to be stored, and into antiresonance with the field mode that is excited through spontaneous Raman scattering driven by the control field interacting with the populated initial state. We have extended previous analyses of cavity-enhanced Λ memories by explicitly considering the evolution of both the Stokes and anti-Stokes fields, and we have derived analytic formulas for the four-wave mixing noise and, a key figure of merit for quantum information applications, the $g^{(2)}$ autocorrelation for the retrieved fields. Our analysis shows that highly efficient and low-noise operation can be simultaneously achieved, and we have presented an example calculation for a memory in Cs vapor which offers the realistic prospect of constructing technically simple quantum memories for near-infrared photons, with near-unit efficiency and negligible noise, operated at GHz rates at room temperature in a chip-scale package powered by diode lasers. We are optimistic that technologies of this kind will enable the field of quantum optics to finally escape the “two-photon doldrums” and explore the physics of large quantum systems.

ACKNOWLEDGMENTS

J.N. acknowledges W. S. Kolthammer and X.-M. Jin for early discussions. This work was supported by the UK Engineering and Physical Sciences Research Council (EPSRC) through the standard Grant No. EP/J000051/1, the programme Grant No. EP/K034480/1, and the EPSRC Hub for Networked Quantum Information Technologies (NQIT). Additional financial support came from the EU IP on Quantum Interfaces, Sensors, and Communication based on Entanglement Integrating Project (Q-ESSENCE; 248095), the Air Force Office of Scientific Research: European Office of Aerospace Research & Development (AFOSR EOARD; Grant No. FA8655-09-1-3020), the EU IP SIQS (600645), and EU Marie-Curie Fellowships No. PIFI-GA-2013-629229 to D.J.S. and No. PIFI-GA-2013-627372 to E.P. C.Q. was

supported by the China Scholarship Council. J.N. acknowledges support from a Royal Society University Research Fellowship. I.A.W. acknowledges an ERC Advanced Grant

(MOQUACINO). M.G.R. and D.V.R. acknowledge financial support from the U. S. National Science Foundation (QIS Program).

-
- [1] A. L. Migdall, D. Branning, and S. Castelletto, *Phys. Rev. A* **66**, 053805 (2002).
- [2] K. McCusker, N. Peters, A. VanDevender, and P. Kwiat, in *Lasers and Electro-Optics, 2008 and 2008 Conference on Quantum Electronics and Laser Science. CLEO/QELS 2008* (IEEE, Piscataway, NJ, 2008), pp. 1–2.
- [3] J. Nunn, N. K. Langford, W. S. Kolthammer, T. F. M. Champion, M. R. Sprague, P. S. Michelberger, X.-M. Jin, D. G. England, and I. A. Walmsley, *Phys. Rev. Lett.* **110**, 133601 (2013).
- [4] R. J. Francis-Jones and P. J. Mosley, [arXiv:1503.06178](https://arxiv.org/abs/1503.06178).
- [5] P. P. Rohde, L. Helt, M. Steel, and A. Gilchrist, *Phys. Rev. A* **92**, 053829 (2015).
- [6] K. Makino, Y. Hashimoto, J.-i. Yoshikawa, H. Ohdan, T. Toyama, P. van Loock, and A. Furusawa, *Sci. Adv.* **2**, e1501772 (2016).
- [7] F. Kaneda, B. G. Christensen, J. J. Wong, H. S. Park, K. T. McCusker, and P. G. Kwiat, *Optica* **2**, 1010 (2015).
- [8] T. Meany, L. A. Ngah, M. J. Collins, A. S. Clark, R. J. Williams, B. J. Eggleton, M. Steel, M. J. Withford, O. Alibart, and S. Tanzilli, *Laser Photonics Rev.* **8**, L42 (2014).
- [9] G. J. Mendoza, R. Santagati, J. Munns, E. Hemsley, M. Piekarek, E. Martin-Lopez, G. D. Marshall, D. Bonneau, M. G. Thompson, and J. L. O'Brien, [arXiv:1503.01215](https://arxiv.org/abs/1503.01215).
- [10] F. Bussi eres, N. Sangouard, M. Afzelius, H. de Riedmatten, C. Simon, and W. Tittel, *J. Mod. Opt.* **60**, 1519 (2013).
- [11] M. Afzelius, T. Chaneli ere, R. L. Cone, S. Kr oll, S. A. Moiseev, M. Sellars *et al.*, *Laser Photonics Rev.* **4**, 244 (2010).
- [12] K. Hammerer, A. S orensen, and E. Polzik, *Rev. Mod. Phys.* **82**, 1041 (2010).
- [13] C. Simon, M. Afzelius, J. Appel, A. B. de La Giroday, S. Dewhurst, N. Gisin, C. Hu, F. Jelezko, S. Kr oll, J. M uller *et al.*, *Eur. Phys. J. D* **58**, 1 (2010).
- [14] A. Lvovsky, B. Sanders, and W. Tittel, *Nat. Photonics* **3**, 706 (2009).
- [15] S. Chen, Y.-A. Chen, T. Strassel, Z.-S. Yuan, B. Zhao, J. Schmiedmayer, and J.-W. Pan, *Phys. Rev. Lett.* **97**, 173004 (2006).
- [16] F. Bussi eres, C. Clausen, A. Tiranov, B. Kozh, V. B. Verma, S. W. Nam, F. Marsili, A. Ferrier, P. Goldner, H. Herrmann *et al.*, *Nat. Photonics* **8**, 775 (2014).
- [17] K. Reim, J. Nunn, V. Lorenz, B. Sussman, K. Lee, N. Langford, D. Jaksch, and I. Walmsley, *Nat. Photonics* **4**, 218 (2010).
- [18] M. Fleischhauer and M. D. Lukin, *Phys. Rev. A* **65**, 022314 (2002).
- [19] K. S. Choi, H. Deng, J. Laurat, and H. J. Kimble, *Nature (London)* **452**, 67 (2008).
- [20] C. Kupchak, T. Mittiga, B. Jorda an, M. Namazi, C. N olleke, and E. Figueroa, *Sci. Rep.* **5**, 7658 (2015).
- [21] J. Nunn, I. A. Walmsley, M. G. Raymer, K. Surmacz, F. C. Waldermann, Z. Wang, and D. Jaksch, *Phys. Rev. A* **75**, 011401(R) (2007).
- [22] D.-S. Ding, W. Zhang, Z.-Y. Zhou, S. Shi, B.-S. Shi, and G.-C. Guo, *Nat. Photonics* **9**, 332 (2015).
- [23] M. Hosseini, G. Campbell, B. Sparkes, P. Lam, and B. Buchler, *Nat. Phys.* **7**, 794 (2011).
- [24] S. Manz, T. Fernholz, J. Schmiedmayer, and J.-W. Pan, *Phys. Rev. A* **75**, 040101(R) (2007).
- [25] N. B. Phillips, A. V. Gorshkov, and I. Novikova, *Phys. Rev. A* **78**, 023801 (2008).
- [26] P. Michelberger, T. Champion, M. Sprague, K. Kaczmarek, M. Barbieri, X. Jin, D. England, W. Kolthammer, D. Saunders, J. Nunn *et al.*, *New J. Phys.* **17**, 043006 (2015).
- [27] N. Lauk, C. O'Brien, and M. Fleischhauer, *Phys. Rev. A* **88**, 013823 (2013).
- [28] M. D abrowski, R. Chrapkiewicz, and W. Wasilewski, *Opt. Express* **22**, 26076 (2014).
- [29] K. Zhang, J. Guo, L. Q. Chen, C. Yuan, Z. Y. Ou, and W. Zhang, *Phys. Rev. A* **90**, 033823 (2014).
- [30] G. Romanov, C. O'Brien, and I. Novikova, *J. Mod. Opt.* **63**, 2048 (2016).
- [31] H. P. Specht, C. N olleke, A. Reiserer, M. Uphoff, E. Figueroa, S. Ritter, and G. Rempe, *Nature (London)* **473**, 190 (2011).
- [32] A. V. Gorshkov, A. Andr e, M. D. Lukin, and A. S. S orensen, *Phys. Rev. A* **76**, 033804 (2007).
- [33] A. Dantan, A. Bramati, and M. Pinard, *Phys. Rev. A* **71**, 043801 (2005).
- [34] Q. Y. He, M. D. Reid, E. Giacobino, J. Cviklinski, and P. D. Drummond, *Phys. Rev. A* **79**, 022310 (2009).
- [35] X.-H. Bao, A. Reingruber, P. Dietrich, J. Rui, A. D uck, T. Strassel, L. Li, N.-L. Liu, B. Zhao, and J.-W. Pan, *Nat. Phys.* **8**, 517 (2012).
- [36] J. Borregaard, M. Zugenmaier, J. M. Petersen, H. Shen, G. Vasilakis, K. Jensen, E. S. Polzik, and A. S. S orensen, *Nat. Commun.* **7**, 11356 (2016).
- [37] D. J. Saunders, J. H. D. Munns, T. F. M. Champion, C. Qiu, K. T. Kaczmarek, E. Poem, P. M. Ledingham, I. A. Walmsley, and J. Nunn, *Phys. Rev. Lett.* **116**, 090501 (2016).
- [38] M. G. Raymer and C. J. McKinstrie, *Phys. Rev. A* **88**, 043819 (2013).
- [39] D. F. Walls and G. J. Milburn, *Quantum Optics* (Springer, New York, 2007).
- [40] D. V. Reddy, M. G. Raymer, and C. J. McKinstrie, *Phys. Rev. A* **91**, 012323 (2015).
- [41] B. Brecht, D. V. Reddy, C. Silberhorn, and M. G. Raymer, *Phys. Rev. X* **5**, 041017 (2015).
- [42] P. Palittapongarnpim, A. A. MacRae, and A. Lvovsky, *Rev. Sci. Instrum.* **83**, 066101 (2012).
- [43] N. B. Phillips, A. V. Gorshkov, and I. Novikova, *Phys. Rev. A* **83**, 063823 (2011).
- [44] C. Wu, M. G. Raymer, Y. Y. Wang, and F. Benabid, *Phys. Rev. A* **82**, 053834 (2010).
- [45] W. Wasilewski and M. G. Raymer, *Phys. Rev. A* **73**, 063816 (2006).

- [46] Q. Glorieux, R. Dubessy, S. Guibal, L. Guidoni, J.-P. Likforman, T. Coudreau, and E. Arimondo, *Phys. Rev. A* **82**, 033819 (2010).
- [47] A. V. Gorshkov, A. André, M. D. Lukin, and A. S. Sørensen, *Phys. Rev. A* **76**, 033805 (2007).
- [48] J. H. D. Munns, C. Qiu, P. M. Ledingham, I. A. Walmsley, J. Nunn, and D. J. Saunders, *Phys. Rev. A* **93**, 013858 (2016).
- [49] Y.-H. Chen, M.-J. Lee, I.-C. Wang, S. Du, Y.-F. Chen, Y.-C. Chen, and I. A. Yu, *Phys. Rev. Lett.* **110**, 083601 (2013).
- [50] W. Wasilewski, T. Fernholz, K. Jensen, L. Madsen, H. Krauter, C. Muschik, and E. S. Polzik, *Opt. Express* **17**, 14444 (2009).
- [51] J. Cirac, L. Duan, and P. Zoller, [arXiv:quant-ph/0405030](https://arxiv.org/abs/quant-ph/0405030).
- [52] J. Nunn, K. Reim, K. C. Lee, V. O. Lorenz, B. J. Sussman, I. A. Walmsley, and D. Jaksch, *Phys. Rev. Lett.* **101**, 260502 (2008).
- [53] A. Eckstein, B. Brecht, and C. Silberhorn, *Opt. Express* **19**, 13770 (2011).
- [54] D. V. Reddy and M. G. Raymer, *Opt. Express* **25**, 12952 (2017).
- [55] D. V. Reddy, M. G. Raymer, C. J. McKinstrie, L. Mejling, and K. Rottwitt, *Opt. Express* **21**, 13840 (2013).
- [56] J. B. Spring, P. S. Salter, B. J. Metcalf, P. C. Humphreys, M. Moore, N. Thomas-Peter, M. Barbieri, X.-M. Jin, N. K. Langford, W. S. Kolthammer *et al.*, *Opt. Express* **21**, 13522 (2013).
- [57] R. Fleischhaker and J. Evers, *Phys. Rev. A* **78**, 051802(R) (2008).
- [58] A. Grodecka-Grad, E. Zeuthen, and A. S. Sørensen, *Phys. Rev. Lett.* **109**, 133601 (2012).
- [59] K. F. Reim, P. Michelberger, K. C. Lee, J. Nunn, N. K. Langford, and I. A. Walmsley, *Phys. Rev. Lett.* **107**, 053603 (2011).
- [60] B. Brecht, K.-H. Luo, H. Herrmann, and C. Silberhorn, *Appl. Phys. B* **122**, 1432 (2016).